Chemical Physics 592 (2025) 112620

Contents lists available at ScienceDirect

Chemical Physics

journal homepage: www.elsevier.com/locate/chemphys

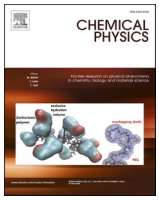

Impact of terminal group on temperature-dependent excited state relaxation in cationic dyes

Yuri Piryatinski [a], Anatoly Verbitsky [a], Markiian Malynovskyi [a], Aleksey Rozhin [b], Oleksiy Kachkovsky [c], Kateryna Maiko [d], Yuri Slominskii [e], Petro Lutsyk [b,*]

[a] Institute of Physics, National Academy of Sciences of Ukraine, Prospekt Nauky 46, 03680 Kyiv, Ukraine
[b] Aston Institute of Photonic Technologies, College of Engineering and Physical Sciences, Aston University, Aston Triangle, B4 7ET, Birmingham, UK
[c] Institute of Bioorganic Chemistry and Petrochemistry, National Academy of Sciences of Ukraine, Murmanska str. 1, 02660 Kyiv, Ukraine
[d] Faculty of Physics, National Taras Shevchenko University of Kyiv, Prospekt Hlushkova 4, 03127 Kyiv, Ukraine
[e] Institute of Organic Chemistry, National Academy of Sciences of Ukraine, Murmanska str. 5, 02660 Kyiv, Ukraine

ARTICLE INFO

Keywords:
Cationic molecules
Time-resolved spectroscopy
Quantum-chemical calculations
Relaxation pathway

ABSTRACT

Cationic organic dyes carry a positive charge distributed along the molecule, and the localization of this charge significantly affects their symmetry and optical properties. Depending on the different factors (topology of the terminal groups, the polarity of the solvent, and the temperature) the polyene, polymethine, or donor-acceptor structure form in such dyes, and excited state relaxation for such systems is not fully explored, particularly at low temperatures. At room temperature, the studied cationic dyes, regardless of symmetry in the ground state, are mostly symmetrical in the excited state. At low temperatures, charge localization effects become evident, leading to symmetry breaking in both ground and excited states. In this paper, we distinguish how terminal groups at the end of the cationic dyes impact the relaxation of excited states by analyzing experimental low-temperature time-resolved spectra combined with quantum-chemical calculations. Distinctive emission (690 nm) in the anti-Stokes range of polymethine band (700–730 nm) features polyene structures forming depending on the temperature, solvent polarity, and charge-donating properties of the dye's terminal groups. Furthermore, in low-temperature time-resolved photoluminescence, a 760 nm band is distinguished and associated with intramolecular charge transfer. Our calculations revealed unequal distribution of total positive charge in different molecular fragments (polymethine chain and terminal groups) and formation of negative charge on polymethine chain. We propose a model of excited state relaxation transitions for linear cationic molecular systems that enable donor-acceptor features. This model offers valuable insights for designing new functional materials with tunable properties or efficient energy transfer systems for artificial photosynthesis.

1. Introduction

Time-resolved spectroscopy is a well-suited practical method for the study of excited state relaxation in the extended conjugated molecules [1,2] with particular interest in tailorable cationic linear polymethine dyes (PMDs) [3–7]. Excitation of such dyes results in their considerable geometrical changes accompanied by the essential electron density redistribution. In cationic PMDs, the positive charge is not located at any single atom but is delocalized in a whole collective π-electron system, generating the solitonic-like charge wave (breather) as well as the corresponding geometrical (or topological) wave [8–11]. It was established experimentally and quantum-chemically that the solitonic waves become mobile in the PMD with a comparatively long polymethine chain; the mobility leads to symmetry breaking, which results in a transformation of a long wavelength band in the absorption spectrum [4,8,12]. It was theoretically predicted that the mobility of such solitonic waves should be sensitive to light excitation. Besides, the geometrical relaxation of the excited molecules is essentially slower and hence it could be investigated by time-resolved spectroscopy [1,2].

Photoluminescence (PL) time-resolved emission spectra (TRES) of PMD with a short carbon chain studied by our group have not revealed substantial changes at room temperature, while at low temperatures (in frozen solutions), the TRES change significantly depending on the temperature and polarity of the solvent in the frozen state [13–15]. One

* Corresponding author.
E-mail address: p.lutsyk@aston.ac.uk (P. Lutsyk).

https://doi.org/10.1016/j.chemphys.2025.112620
Received 22 October 2024; Received in revised form 10 January 2025; Accepted 23 January 2025
Available online 27 January 2025

of manifestations of these changes is the appearance of PL in anti-Stokes range of polymethine structure in the spectra [15], as well as the broadening and strengthening of the absorption bands in the region of the first electron-vibrational transition. It was established that charge and geometrical wave can shift from the chain center to one of the terminal groups (TGs) resulting in the symmetry breaking. This effect depends essentially on molecular topology of TGs, which was comprehensively analyzed in the ground state (absorption spectra) [5,12,16], but there is a knowledge gap in excited state relaxation, particularly more in-depth understanding of the PL the anti-Stokes range. At the same time, it was shown that length of the solitonic waves in excited state is essentially shorter [17]. Therefore, symmetry breaking in the excited state seems to occur in the dyes with shorter polymethine chain, and this effect should depend on chemical constitution of the TGs. Earlier [15], we reported on excited state relaxation of the **pyrylocyanine** (**PyC**) dye (Fig. 1a) and showed the shifts of atomic charges to a TG upon excitation. Here, we comparative study another cationic dye (Fig. 1b) containing the TGs with ability to donate the π-electron density from them to the atoms of the polymethine chain, with the aim to understand an impact of TG features on symmetry breaking of the dye. In **PyC** dye (Fig. 1a), the TGs are virtually prolongation of the polymethine chain (branched polymethine chain). In **benzo[*e*]indocyanine (BIC) dye** (Fig. 1b), the open polymethine chain is the same, whereas both TGs contain own cyclic π-electron systems conjugated with the open polymethine chain via nitrogen-containing groups. Thus, both dyes have typical for PMDs structure shown by formula (1):

$$\left[\mathrm{TG}\text{–}(\mathrm{CH})_n\text{–}\mathrm{TG}\right]^+ \quad (1)$$

where $(CH)_n$ is open polymethine chain.

Pyrylium TGs in PyC can be treated as low electron density donating group, whereas BIC TGs would be able to transfer electron density to the polymethine chain [5]. Changing donor properties of TGs will significantly influence the charge distribution in the open polymethine chain. The main aim of this study is to evaluate the impact of TGs induced charge distribution on electronic properties and relaxation processes of cationic dyes via low-temperature time-resolved fluorescence analysis and quantum-chemical modelling. Furthermore, strong redistribution of electron density results in the emergence of a large dipole moment, and consequently appearance of such features, like two-photon absorption, up-conversion, energy transfer, etc., thus, as an outcome, efficient nonlinear optical properties can be designed and modelled in such molecular systems

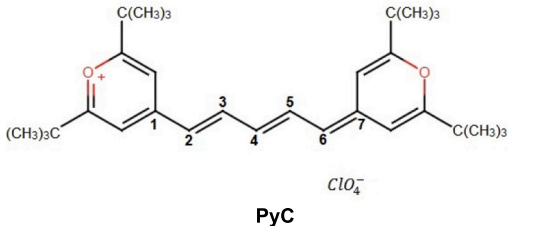

Fig. 1. Chemical structure of the studied **PyC** and **BIC** dyes with enumeration (μ) of carbon atoms in the polymethine chain.

2. Experimental

Chemical structure of studied **PyC** and **BIC** dyes is shown in Fig. 1. Both dyes constitute of cationic conjugate and ClO_4 counter anion. The synthesis of these dyes was described earlier [18], and the purity of the dyes of ≥98 % was determined by liquid chromatography-mass spectrometry technique. Acetonitrile and toluene solutions of the dyes were studied.

The absorption spectra were measured using Shimadzu UV-3100 spectrometer. Spectra of steady-state photoluminescence (PL) were recorded by both a USB2000 + UV-VIS-ES spectrometer supplemented by 600-μm-diameter optical fiber (Ocean Optics B.V.) and by a LifeSpec II spectrofluorometer (Edinburgh Instruments Ltd). The PL has been excited by an MGL-F-532-1.5 W laser (CNI Optoelectronics Tech. Co., Ltd) having a maximum of excitation wavelength at λ_{EX} = 530 nm.

Time-resolved PL emission spectra (TRES), kinetics of PL, and TRES maps were measured by a LifeSpec II spectrofluorometer (Edinburgh Instruments Ltd) applying time-correlated single-photon counting (TCSPC) technique. TRES maps were obtained by recording multiple PL kinetics for various PL emission wavelengths, λ_{EM}, and as outcome, such map represent PL intensity versus λ_{EM} and delay time. In this case, PL was excited by an EPL-405 and EPL-670 ps pulsed diode lasers (Edinburgh Instruments Ltd) with λ_{EX} = 405 nm and 675 nm, respectively. Measurements with these two λ_{EX} ensures no contributions from higher excited states [19] in our spectral analysis. F900 software package (Edinburgh Instruments Ltd) was used for identification of the lifetimes of excited states, which allows to extract the lifetimes as short as 1/10th of the system's Instrumental Response Function (IRF) due to numerical reconvolution. Colloidal LUDOX solution was used to obtain the IRF.

The quantum-chemical calculations were performed using the GAUSSIAN09 package [20] aiming to study features of electronic structure and electron transitions of the dyes. Considering that only the π-electron system defines the main properties of the dyes, the bulky tert-butyl substituents of the TGs were substituted by methyl groups (CH_3) in the calculations, which were performed in vacuum. The optimization in the ground state was performed by the non-empirical *DFT* method with *6-31G(d,p)* basis set and *B3LYP* functional. The geometry in the excited state and the electron transition characteristics were calculated by the non-empirical *TD-DFT* method (with the same basis set and functional; the choice of functional does not influence qualitatively the charge wave in studied molecules [21]; however, B3LYP is considered to have significant shortcomings in correct description of charge transfer states [22]). Mulliken charges has been analyzed. As a note, the calculated and the experimental data have no ideal matching being a typical outcome for such systems [23], but the calculated data is sufficiently accurate for appropriate analysis of attributes in the studied molecules.

3. Results and discussion

3.1. Molecular geometry and electron structure

Main electronic properties and long wavelength absorption of studied dyes are related to electron structure of polymethine chain in both ground and excited state. The TGs give some perturbation causing additional bathochromic shift of the first spectral band and shifting the electron levels, particularly, the frontier levels involving in the lowest electron transition upon excitation. In both dyes, TGs contribute substantially to the total molecular orbital's delocalization (Fig. S1, Table S1), and the total positive charge (Mulliken charges) is distributed unequally in the different molecular fragments of the **PyC** and **BIC** dyes in the ground and excited state (see Table 1).

One can see from Table 1 that the total positive charge is delocalized at both pyrylium TGs and the chain of the **PyC** dye. However, most of the charge is localized at the TGs with minimal part on the chain. For **BIC** dye, the polymethine chain has a negative charge in both ground and excited state, so that both TGs transfer excess of the electron density to

Table 1
Fragmentary charge (q) distribution on TG_1, the polymethine chain (-CH=CH-CH=CH-CH=), TG_2 and charge transfer to the chain upon excitation: $S_0 \rightarrow S_1$ (Δq).

Dye	State	$q(TG_1)$]	q(chain)	$q(TG_2)$	Δq
PyC	S_0	+0.498	+0.004	+0.498	**+0.034**
	S_1	+0.481	+0.038	+0.481	
BIC	S_0	+0.524	−0.048	+0.524	**−0.082**
	S_1	+0.565	−0.130	+0.565	

the chain. The excitation ($S_0 \rightarrow S_1$) is accompanied by partial redistribution of electron density between molecular fragments: positive charge transfers from the TGs to the chain in the **PyC** dye ($\Delta q = +0.034$), whereas negative charge increases on the chain in the **BIC** dye ($\Delta q = -0.082$). One of the reasons of electron density transferring to the chain in BIC molecule could be a nature of nitrogen-carbon interaction, which attracts high positive charge to carbon atoms at $\mu = 1,7$ and brings negative charges to neighboring carbons, $\mu = 2,6$, respectively (Fig. 2a).

Furthermore, the charges at the adjacent carbon atoms in the open polymethine chain alternate, being typical for the PMDs [3,5,7]. The excitation ($S_0 \rightarrow S_1$) causes considerable charge redistribution at the chain atoms. The charge redistribution is alternated at the adjacent atoms. This alternation could be presented as solitonic-like wave of values Δq_μ, calculated by formula (2):

$$\Delta q_\mu = q_{\mu+1} - q_\mu \quad (2)$$

where q_μ - is the electron density change at the μ-th carbon atom. The alternation waves for both dyes presented on Fig. 2. The charge alternation at both chain ends is sensitive to the chemical constitution of TGs.

Besides, the alternation of bond length along PMD chain defined as, $\Delta l_\nu = l_{\nu+1} - l_\nu$, where l_ν is bond length of ν-th bond, appears in the chain of studied symmetrical PMDs, but this alternation increases from chain center to both chain ends (Fig. S2). Such result is contrasting to Δl_ν of typical polyenes, where bond length alternation appears from one end of the chain to another chain end (along whole chain). The Δl_ν amplitude is sensitive to TGs, similarly to sensitivity of charge alternation (Δq_μ). Thus, the electron structure of open chain is highly sensitive to studied TGs differing with ability to transfer electron density to the chain.

Temperature dependences of absorption and steady-state photoluminescence (PL) spectra.

Absorption and steady-state PL spectra of the **PyC** (Fig. 3a,c) and **BIC** (Fig. 3b,d) dyes were studied in the highly polar acetonitrile (Fig. 3a,b) and nonpolar toluene (Fig. 3c,d) solvents. The wavelengths of absorption maxima (λ_{abs}^{max}), PL emission maxima (λ_{EM}^{max}), and Stokes shifts ($\Delta\lambda_S = \lambda_{EM}^{max} - \lambda_{abs}^{max}$) summarized in Table 2. At 296 K, λ_{abs}^{max} and λ_{EM}^{max} for **PyC** (Fig. 3a,c) are slightly changing at various solvents, whereas the peak positions for **BIC** (Fig. 3b,d) are practically the same for studied solutions. The Stokes shift ($\Delta\lambda_S$) featuring redshift of the emission peak (λ_{EM}^{max}) relatively to the maximum of absorption (λ_{abs}^{max}) is quite small, which is characteristic to PMDs [20].

Furthermore, the spectra were measured at low temperatures (4.2 and 77 K), when the solutions are in the solid-state (Fig. 3). In low-temperature (77 K) absorption spectra for the symmetric **PyC** dye, a broadening and increase in the intensity of the bands in the range of the electronic-vibrational 0–1 transition is observed in comparison to the room-temperature spectra Fig. 3a,c). This can be associated with the existence in frozen solutions of **PyC** dye molecules with broken symmetry (polyene structure) and significant alternation of single and double bonds. A significant change in bond lengths upon excitation of asymmetric dyes usually leads to strengthening of vibrational interactions and broadening of absorption bands [24]. In our case, the broadening and increase in the absorption intensity in the range of the electronic-vibrational 0–1 transition can be associated with the superposition of the absorption bands of polymethine and polyene forms. Furthermore, comparing low-temperature absorption spectra of **PyC** (Fig. 3a,c) and **BIC** (Fig. 3b), it is evident that for **PyC** these changes in the range of the 0–1 electron-vibrational transition are significantly greater than for **BIC**.

In low-temperature steady-state PL spectra of **PyC** dye (Fig. 3a,c), in addition 0–0 transition peak, 690 nm band is registered falling into the anti-Stokes region. This band is positioned above the lowest 0–0 optical transitions for solutions of the symmetric form of **PyC**, has very low intensity in acetonitrile (Fig. 3a) and relatively high intensity in toluene (Fig. 3c, curve 4). The nature of this band cannot be associated to the effect of optical cooling, or from the point of view of the violation of the Kasha rule. The emergence of the 690 nm PL band correlates with the absorption spectra changes in the region of the electron-vibrational 0–1 transition. 690 nm PL can be associated with the emission of **PyC** molecules with broken symmetry (polyene structure) in frozen solutions. Different intensities of the 690 nm band in acetonitrile and toluene evidence that there is higher contribution of **PyC** molecules with broken symmetry in nonpolar toluene than in highly polar acetonitrile.

Furthermore, the emission component associated with the 690 nm band predominates in the low-temperature (77 K) steady-state PL spectra of the acetonitrile solution of **BIC** dye (Fig. 3b). Thus, **BIC** dye transforms into non-symmetric polyene structure at low temperature. Predominance of such polyene structure for BIC dye can be attributed to electron density transferring from the TG to the chain in **BIC** molecule (Table 1, Fig. 2). For the nonpolar toluene solution, the steady-state PL

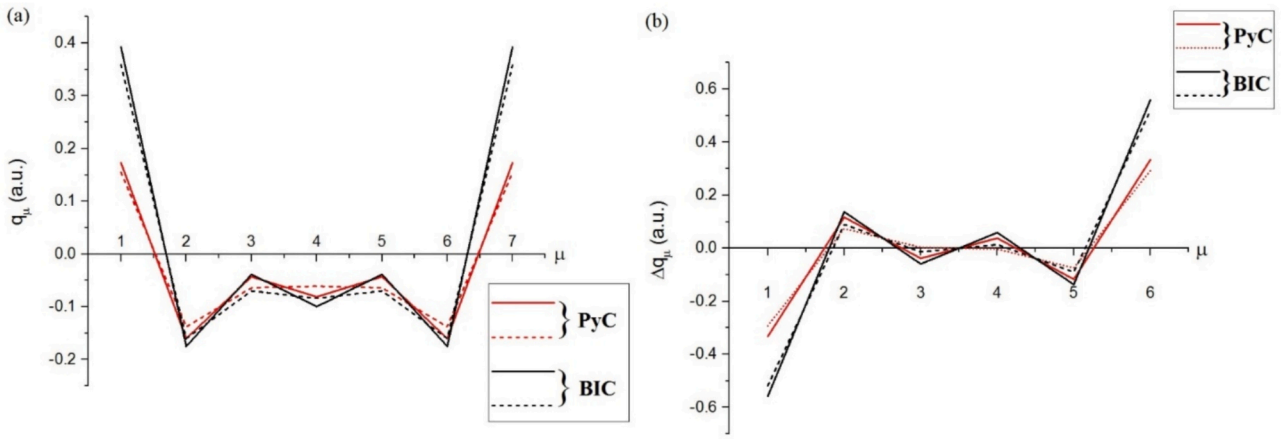

Fig. 2. (a) Atomic charges, q_μ, and (b) alternation of atomic charges, Δq_μ, on the carbon atoms of the polymethine chain in **PyC** (red) and **BIC** (black) dyes; solid lines are attributed to the ground state, and dashed lines (– – -) are representing the excited state. (For interpretation of the references to colour in this figure legend, the reader is referred to the web version of this article.)

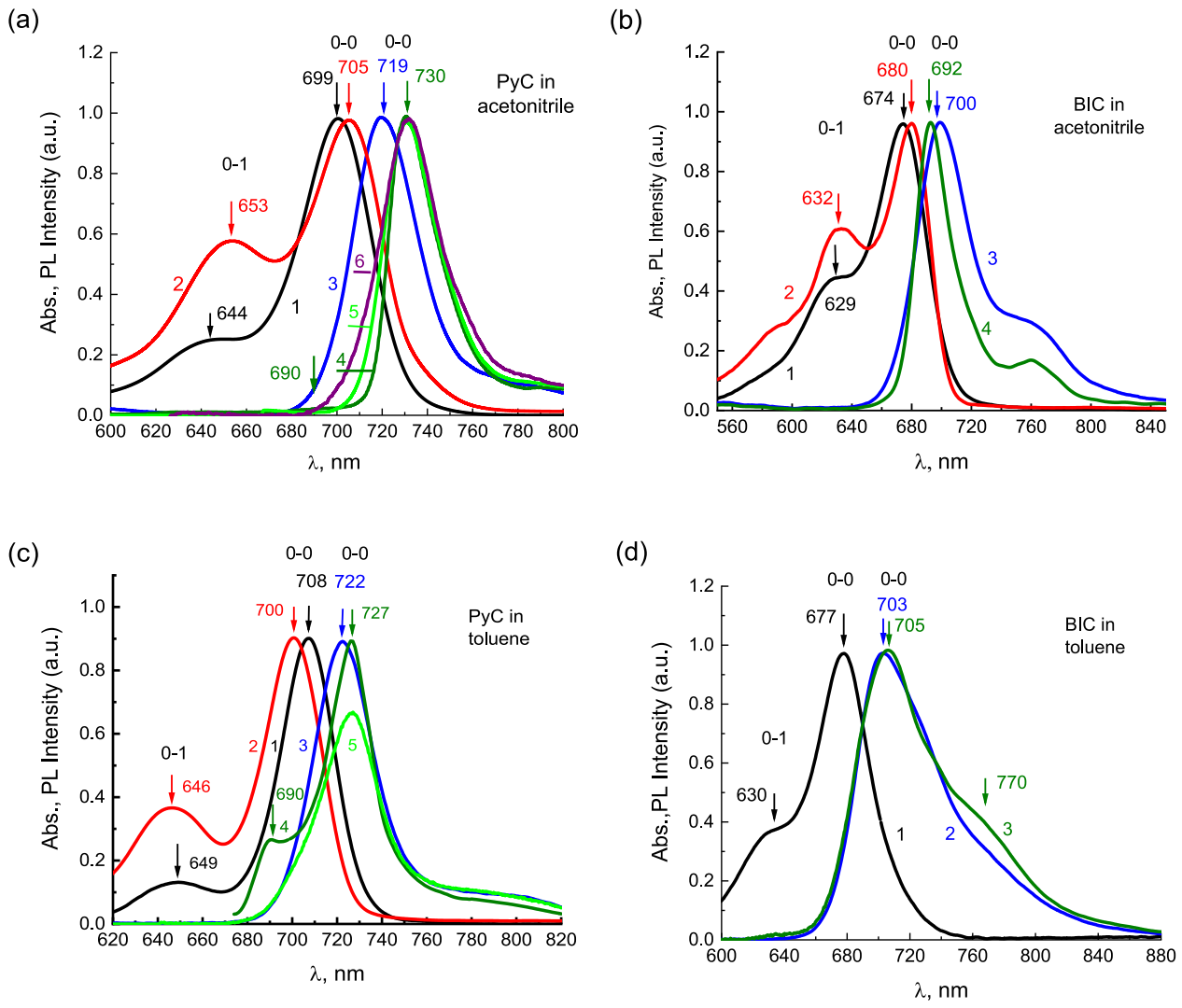

Fig. 3. (a) Absorption (1,2) and steady-state PL (3–7) spectra of the **PyC** in acetonitrile at 296 K (1,3), 77 K (2), 4.2 K (4), 110 K (5) and 190 K (6). (b) Absorption (1,2) and steady-state PL (3,4) spectra of the **BIC** in acetonitrile at 296 K (1,3) and 77 K (2,4). (c) Absorption (1,2) and steady-state PL (3–5) spectra of the **PyC** in toluene at 296 K (1,3), 4.2 K (4), and 170 K (5). (d) Absorption (1) and steady-state PL (2,3) spectra of the **BIC** in toluene at 296 K (1,2) and 77 K (3).

Table 2
Absorption maxima (λ_{abs}^{max}), PL emission maxima (λ_{EM}^{max}), and Stokes shift ($\Delta\lambda_S$) for the **PyC** and **BIC** dyes.

Dye Solvent	296 K			77 K		
	λ_{abs}^{max}, nm	λ_{EM}^{max}, nm	$\Delta\lambda_S$, nm	λ_{abs}^{max}, nm	λ_{EM}^{max}, nm	$\Delta\lambda_S$, nm
PyC in acetonitrile	699	719	20	705	730	25
PyC in toluene	708	722	14	700	727	27
BIC in acetonitrile	674	700	26	680	692	12
BIC in toluene	677	703	26		705	

spectra (Fig. 3d) do not change significantly upon going from room temperature to 77 K. In the low-temperature PL spectra of **BIC** dye, a small increase in the intensity of the 770 nm band is observed.

The temperature dependence of steady-state PL spectra of the **PyC** dye in acetonitrile solutions has been analyzed (Fig. 3a) from room temperature (liquid solution) to 4.2 K (solid solution). The melting point of acetonitrile solution is 228 K. In the temperature range of 4.2–60 K, the shape and intensity of the PL band with a maximum at 730 nm do not change. At further increase of temperature, the intensity of the PL drops, and the band become broader. In Fig. 3a, the spectra are presented in a normalized form, and such normalization shows that the spectra at 4.2 K are the narrowest comparing to higher temperatures. The greatest broadening of the PL bands was observed at temperatures close to the melting temperature of the solution. Analysis of steady-state PL spectra at various intermediate temperatures indicates that a purely electronic emission band can be represented as a superposition of two PL bands - a high-temperature one (typical for a liquid solution at 296 K) and a low-temperature one (typical for temperatures of 4.2–60 K). At temperatures above 60 K, the contribution of the low-temperature component decreases, and the high-temperature component start to increase.

Low-temperature (4.2–60 K) PL spectra of **PyC** dye solutions in nonpolar toluene have a maximum at 727 nm, associated with emission from the lowest excited state of the molecule, and an intense anti-Stokes band at 690 nm. This band can be associated with emission from molecules with broken symmetry in the charge distribution in the ground state and significant alternation of bond lengths in the carbon chain. With an increase in temperature to 170 K, the 690 nm band disappears. The intensity of the 727 nm band decreases without significant changes in the position of its maximum and shape for a solid solution of **PyC** in toluene in the temperature range of 60–18 K. At temperatures above 100 K the emission spectrum of **PyC** molecules can be represented as a superposition of the low-temperature (4.2–60 K) and high-temperature

(liquid solution) emission components. In the case of toluene solution of **PyC**, the contribution of the high-temperature PL component to the 727 nm PL band is significantly smaller than for **PyC** in polar acetonitrile. Thus, at low temperatures (4.2–60 K) **PyC** molecules in toluene has both: symmetrical in the ground state (727 nm band) and nonsymmetric (690 nm band). At room temperature, liquid solution of **PyC** in toluene has mainly symmetrical molecules. Therefore, studying frozen solutions allows us to observe transition of **PyC** molecules from a symmetrical form to an asymmetrical one and vice versa.

3.2. Time-resolved emission spectra (TRES) maps and relaxation dynamics

Fig. 4 shows the low-temperature TRES spectra for **PyC** in acetonitrile and toluene. The 692 nm band is observed in the low-temperature time-resolved PL spectra of **PyC** solutions. Same way as steady-state spectra, the low-temperature TRES has the anti-Stokes 692 nm peak much higher for nonpolar toluene that for polar acetonitrile solutions. Moreover, with an increase in t_d from 5600 to 14,000 ps, a new band peaking at 770 nm appears. The new 770 nm band largely depends on the frozen solvate shell of the dye: it appears in polar acetonitrile (Fig. 4a) and is practically not visible in nonpolar toluene media (Fig. 4b). The strongest and fastest changes in the PL spectra occur in the anti-Stokes 692 nm band in the range of delay times t_d = 50–7000 ps. It should be noted that 692 nm band is best featured in the fast time-resolved spectra (i.e. t_d = 50 ps). The PL lifetimes (Tables S2-S4) are determined from the exponential fitting of the measured PL decays for studied solutions of the **PyC** and **BIC** dye; besides, the PL lifetimes and TRES maps for **PyC** dye in acetonitrile are analyzed in our previous publication [15].

Fig. 5a,b shows the TRES maps for acetonitrile solution of **BIC** dye. The wavelength of the TRES excitation laser λ_{EX} = 675 nm falls into the spectral region close to the excitation energy of the lowest electron 0–0 transitions of both symmetric and asymmetric forms of the dye. The room-temperature TRES map for **BIC** dye (Fig. 5a) shows that the shape of instantaneous PL spectra (peaking at 697 nm) remains practically unchanged at different t_d = 0–6 ns. The low-temperature (4.2 K) TRES map of **BIC** dye (Fig. 5b) evidences fast changes occurring after excitation up to 2 ns. In addition to PL maximum at 690–695 nm, a small band with a maximum at 770 nm emerges on the low-temperature TRES map, which is not present in the room-temperature TRES map. Figs. 5c,d show low-temperature (4.2 K) TRES spectra for **BIC** dye in acetonitrile. The fastest changes for **BIC** occur in the range of 680–700 nm. In the differential PL spectrum (Fig. 5c), get by subtracting 900 ps curve from the 6300 ps curve, the band with maximum at 690 nm is revealed. At t_d varying from 5600 to 14,000 ps (Fig. 5d), the most dramatic change of PL is happening in the range of 720–800 nm. A new band peaking at 770 nm emerged in the PL spectrum at t_d = 6000–14,000 ps. The PL lifetime for this band is about 3850 ps at 4.2 K and 3520 ps at 77 K (Table S3). It needs to be noted that highly intensive 770 nm peak is much dependent on the frozen solvate environment: emerging in polar acetonitrile and practically not appearing in nonpolar media of toluene (Fig. 3d).

The emission bands in the range of 690 nm are better distinguished in the TRES spectra at short delay times (Figs. 4,5) t_d < 1 ns and can be associated with purely electronic transitions, characteristic for polyene-type carbon chain molecular structures. For **BIC**, the lifetimes of these bands at 4.2 K are τ_1 = 227 ps and τ_2 = 1610 ps (Table S3). The PL component with τ_1 = 227 ps can be associated with relaxation processes in the 690 nm band, and the component with τ_2 = 1610 ps would be a contribution of the intense band at 700 nm overlapping with the 690 nm band.

At long delay times (> 5 ns) (Fig. 5), a new emission band appears in the long-wavelength region of TRES at 770 nm, which cannot be attributed to a vibronic transition. The intensity of this band is much higher for the **BIC** compared to the **PyC** dye, which can be attributed to ability to transfer the π-electron density from the TGs. The lifetime for this band at 4.2 K is τ_2 = 2470 ps and τ_3 = 3850 ps, where slowly decaying PL (τ_3) can be associated with relaxation processes in the 770 nm band, and the intermediate component with τ_2 = 2470 ps is attributed to the contribution of the intense 700 nm band still overlapping with the 770 nm band. The 690 and 770 nm bands are well separated in the TRES with different time delays (Fig. 5c,d and Fig. S3).

3.3. Temperature-dependent solvatochromism in excited state relaxation

Relaxation of the dye molecule from excited to the ground state can result in the alterations of its structure, e.g., torsion angles. Measurements of PL spectra at low temperature (4.2 and 77 K) allows us to factor out the impact of torsion changes on the electronic structure of the dye in the excited state. Such low-temperature solutions are frozen to the solid state, so any structural changes in the molecules are subdued, and the distribution of the dyes by symmetry is preserved in their solvate

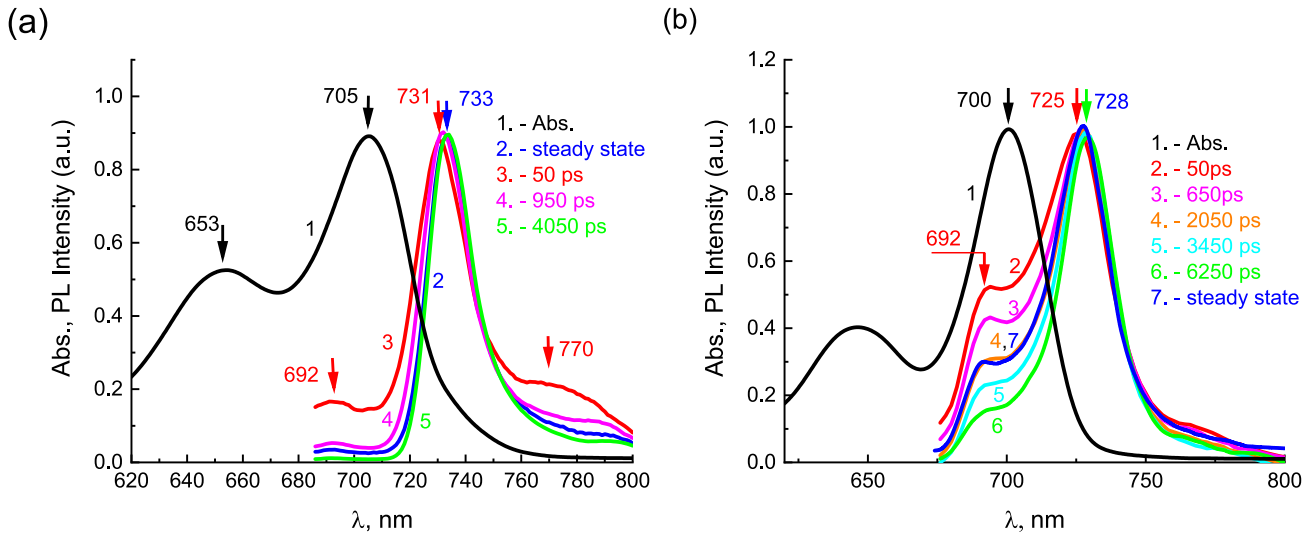

Fig. 4. (a) Absorption (1), steady-state PL (2) spectra and TRES (3–5: t_d = 50 (3), 950 (4), 4050 (5) ps) of the **PyC** in acetonitrile at 77 K (1) and 4.2 K (2–5). Steady-state PL spectra and TRES are normalized to the peak of the most intense band with maximum at approx. 733 nm; λ_{EX} = 405 nm.
(b) Absorption (1), steady-state PL (7) spectra and TRES (2–6: t_d = 50 (2), 650 (3), 2050 (4), 3450(5) and 6250 (6) ps) of the **PyC** in toluene at 77 K (1) and 4.2 K (2–7). Steady-state PL spectra and TRES are normalized to the peak of the most intense band with maximum at approx. 728 nm; λ_{EX} = 405 nm.

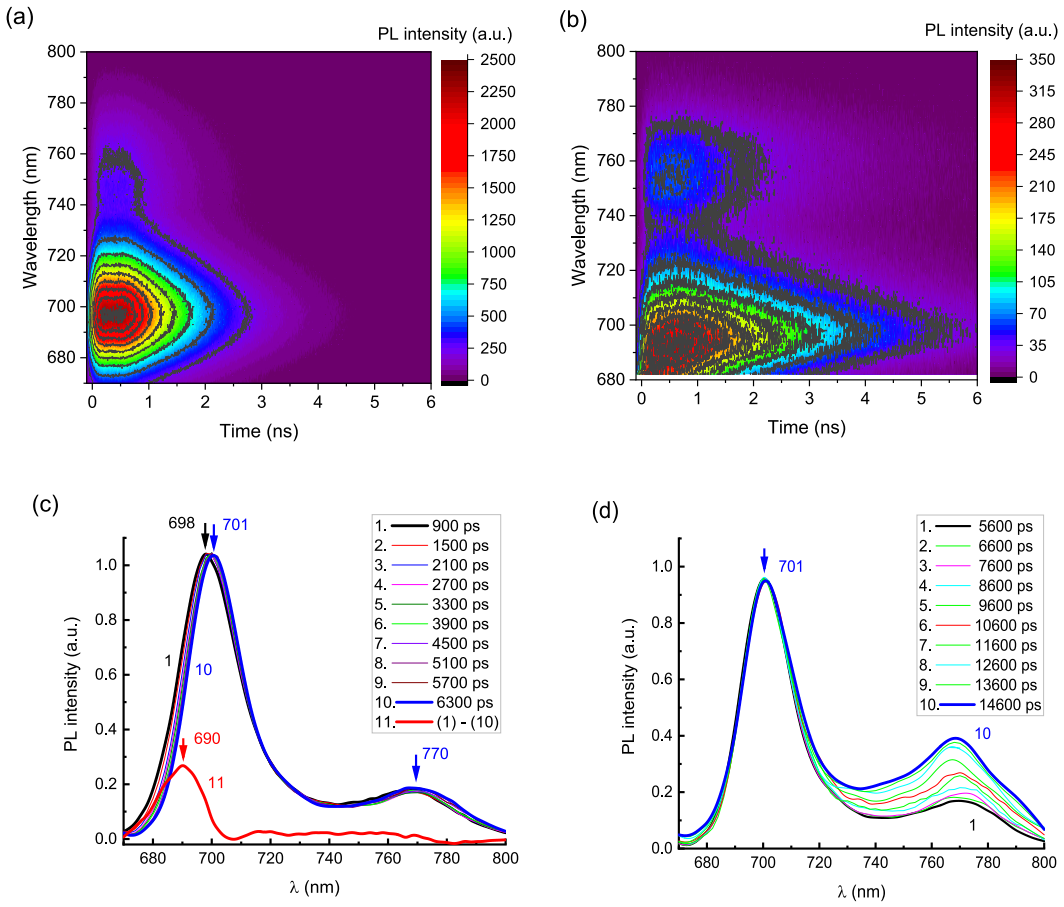

Fig. 5. (a,b) TRES maps for acetonitrile solutions of **BIC** dye at 296 K (a) and 4.2 (b) K; λ_{EX} = 675 nm. (c,d) TRES normalized at approx. 701 nm (the most intense band) at λ_{EX} = 405 nm for acetonitrile solution of **BIC** at 4.2 K (c) in the range of t = 900–6300 ps with 600 ps increment (curves 1–10) and (d) in the range of t = 5600–14,600 ps with 1000 ps increment (curves 1–10). Differential TRES (curve 11) is obtained by subtracting curve 10 (t = 6300 ps) from curve 1 (t = 900 ps) in part (c).

shell. The low temperature solvation shell of the molecule does not follow-up the charge changes at the optical excitation. Therefore, the dye in the excited state stays in the electric field of the ground state solvation shell. $\Delta\lambda_S$ at 77 K (Table 2) reflects the molecule in the frozen solvation shell, and for **BIC** dye there is a dramatic decrease of $\Delta\lambda_S$ from 28 to 12 nm in polar acetonitrile (whereas **PyC** $\Delta\lambda_S$ slightly increases from 20 to 25 nm). Such behavior can be attributed to different Δq distributions (Table 1) affected by TG, and further studies for diverse range of the dyes is underway aiming to provide more in-depth insight on such changes.

The symmetry breaking in cationic dyes, associated with the charge distribution in the carbon chain in the ground and optically excited states, is significantly affected by the solvent polarity and ambient temperature. In the temperature range from 4.2 K to solvent's melting point, the solvent is in the solid-state. At low temperatures, the charged dye molecules remain in the solvation shell that they had at room temperature. The polarity of the charges on the carbon atoms of the dye molecules changes during the optical transition to the excited state. In this case, the repulsive potential of the charges of the solvation shell, which is strongest in the center of the carbon chain, acts on the charged carbon atoms in frozen solutions. The electric field of the charges in the solvation shell can change the distribution of charges in the carbon chain and the symmetry of this distribution. In such electric field, the polaron in an excited state of a molecule can expand from the center to the TGs, thereby changing the alternation of charges and bond lengths along the carbon chain. For nonpolar toluene solutions of dye, the PL spectra are mainly influenced by electronic polarization at both room and low temperatures (liquid and solid solution, respectively). In this case, smaller changes in the electron density distribution would occur comparing to the system of the molecules in polar acetonitrile.

At room temperature, the interaction between charged molecules of cationic dyes and the solvation shell of a polar solvent in the ground and excited states is attributed to electronic and reorientation polarizations. In solid solutions, the reorientation of the solvent molecules is absent thus the reorientation polarization associated with this is minimized. The PL spectra at low temperatures are affected mostly by electronic polarization. Besides, the ground state distribution in frozen solvent and, thus, PL depend on the solvent polarity. In a nonpolar solvent, the cationic dye in the excited state interacts with solvent through electronic polarization in solid and liquid states. Polarons in the carbon chain are mobile and this can lead to reduced symmetry in the distribution of electron density and the equilibrium geometry of molecules, and as a result broadening of the absorption spectra is observed [25]. The symmetry breaking affects the charge distribution in PMDs [26,27]. The symmetry breaking in PMDs with a long carbon chain leads to the appearance of a new absorption band in the short-wavelength region of the spectrum. In studied pentamethine dyes having relatively short polymethine chain, the new 690 nm PL is associated with the emission of molecules with broken symmetry in frozen solutions. Besides, the contribution of **PyC** molecules with broken symmetry in nonpolar toluene is higher than in highly polar acetonitrile. As shown by quantum chemical calculations, the symmetry breaking for **PyC** molecules in the ground state in a nonpolar solvent can be associated with the localization of the counterion at one of the TG and the shift of the polaron to TG [28]. The localization of the polaron at one of the TG of the dye, leading to symmetry breaking in the charge distribution in the molecule, is

attributed to molecular vibrations and solvent effects. Furthermore, the features of the band at 690 nm correlate with the absorption spectra analysis for long-chain cyanine dyes [29], where asymmetric molecules with blue-shifted spectra form in nonpolar toluene comparing to symmetric molecules in highly polar solvent.

Depending on the environment of the studied molecules and temperature, the excess charge in the molecule can be localized in different proportions in the center of the carbon chain and near the TGs. For liquid molecular solutions of **PyC** in acetonitrile, the maximum in the distribution of excess charge in the dye molecule is concentrated in the center of the carbon chain, and PL occurs mostly without breaking symmetry. Therefore, it can be assumed that there are two types of symmetric states for polar acetonitrile solutions of **PyC** at different temperatures - high-temperature (Figure 3a, curve 3) and low-temperature (typical for temperatures of 4.2–60 K). For low-temperature symmetric phase in the electric field of a frozen solvation shell, the excess mobile charge distribution has maxima in the center of the chain and near the TGs. With different ratios of the localization of excess charge near the TGs, symmetry breaking in the ground state is observed [25]. In this case, PL from low-temperature symmetric states is observed (PL bands at 730 nm) and states with broken symmetry (PL bands at 690–693 nm). In the excited state, molecules with broken symmetry can transform into symmetric ones due to charge tunneling or an activation process. Besides, it has been established in our previous work [15] that the π-conjugated carbon chain of **PyC** with a positive charge localized on it plays the main role in the processes of optical electronic excitation and excitation relaxation processes, while the impact of TG is weak. The symmetric and nonsymmetric localization of the cationic charge on the carbon chain between the TG was considered being close to the polymethine and polyene conformations, respectively. The relaxation processes for the **PyC** dye were explained in terms of the free electron model followed by the formation of large radius polarons. The effect of symmetry breaking on the electronic properties of the **PyC** dye was considered for transition from polymethine to polyene in the ground and excited states. The polyene structure of the carbon chain of the **PyC** dye could be obtained in a nonpolar solvent in the case of charge localization on one of the TGs. To analyze the relaxation pathways of electronic excitation in polyene structures, the molecular exciton model can be used [15]. Thus, such modelling can be applied to the pentamethine molecules with low electron density donating TGs, like pyrylium TGs.

Our quantum-chemical calculations (Table 1) shows that the **BIC** molecule is symmetrical, and a small fraction of the negative charge is localized on the carbon chain. The excess positive charge is equally localized on the TGs. This charge distribution in the **BIC** dye shows the predominantly polyene structure of the carbon chain in the ground state and the associated optical absorption of the molecule. The **BIC** molecule, with a localized positive charge on the TG and some fraction of the negative charge on the carbon chain, can be represented as a bichromophore (donor-acceptor-donor, D-A—D, bis-dipole [30]) structure with a common π-conjugated acceptor. For cationic molecule, the D-A-D structure should be represented as $(D\text{-}A\text{-}D)^{+}$. In the excited state **BIC** molecule, the intramolecular negative charge transfers from TG to the carbon chain (Table 1), which also changes the donor–acceptor interaction within the chromophore and between them. Depending on the degree of intramolecular interaction, PL can involve a nonsymmetric polyene form of the **BIC** molecule with intramolecular charge transfer (ICT) and localization of the D-A radiative transition on one of the TGs and the carbon chain, or a polymethine form of the **BIC** molecule with localization of excitation on the carbon chain (Fig. S1). Our results are in corroboration with study of PMDs having central substituents with various electron-donating character, where strong electron-donor groups create bis-dipole structures with significantly changed spectral properties [30].

The presence of nodes in the inhomogeneous distribution of charges (Fig. 2) and bond lengths (Fig. S2) on the carbon chain in the ground state, at low temperatures, creates potential barriers for conjugation of the D-A chromophore and their interaction. The chromophores conjugation and interaction are enhanced upon optical excitation of the **BIC** molecule due to the photoinduced transfer of the negative charge from the TGs to the carbon chain. The localization of an excess negative charge on the carbon chain leads to an additional equalization of bond lengths (Fig. S2) and expansion of the conjugation region due to a decrease in the barriers. Such a supramolecular structure can also be considered as a molecular dimer of polar chromophores and their dipole moments increase significantly due to the high electron density donating of TG in the excited state [31].

The molecules in the excited state with ICT can be presented as a sum of a neutral locally excited state with main excitation on the chain $(D\text{-}A^{*}\text{-}D)^{+}$ and two degenerate charge transfer (CT) states $(D\text{-}A^{-}\text{-}D^{+}$ and $D^{+}\text{-}A^{-}\text{-}D)$. Instantly after the optical excitation, the molecular system most likely would be in the $(D\text{-}A^{*}\text{-}D)^{+}$ excited Franck-Condon state. After some time, the fluorescent CT states (770 nm band) appears. These CT states have significant $\Delta\lambda_S$, which can be associated with the symmetry breaking in the charge redistribution along the molecule during its optical excitation. The ICT state induced by the local excited state interacting with one of the TGs is one of the explanations for the appearance of this band [32]. In PMD molecules having carbon chain/TG with different electron/hole affinities, the excited state tends to obtain charge transfer features, where electrons and holes are separated on these different molecular parts and can participate in subsequent radiative processes.

The formation of a $D\text{-}A^{-}\text{-}D^{+}$ molecular structure can be explained by the emergence of a band at 770 nm with a lifetime of 3850 ps, which appears at long delay times for the **BIC** dye in a polar solvent. The intensity of this band strongly depends on the ability of TG to transfer electron density to the chain. For the **PyC** dye, the distinctive band at 770 nm is not observed (except some short time features in the differential spectra [15]). This band is not observed in the absorption spectra of the **BIC** dye, since it is formed due to exciton absorption in the polyene structure, it could be followed by photoinduced charge transfer (tunneling) from TG to the carbon chain and interaction between D-A chromophores. This mechanism is confirmed by the long delay times in its appearance. If the band appeared due to direct excitation of the $D^{+}\text{-}A^{-}$ state, then the delay time would correlate with time of direct excitation being in the range of femtoseconds. Therefore, after optical excitation, a molecular exciton could be formed in the **BIC** molecule with the polyene chain structure, $(D\text{-}A^{*}\text{-}D)^{+}$. Such exciton migrates along a one-dimensional carbon chain, quickly self-localizes without a barrier, and such self-trapped exciton can be observed in the PL spectra [33,34]. The interaction of an excited state with the near-terminal region having a different electron affinity promotes ICT between TG and the carbon chain $\{(D\text{-}A\text{-}D)^{+}\}^{*} \rightarrow (D\text{-}A^{*}\text{-}D)^{+} \rightarrow (D\text{-}A^{-}\text{-}D^{+}$ or $D^{+}\text{-}A^{-}\text{-}D)$. This leads to symmetry breaking $(D\text{-}A^{*}\text{-}D)^{+} \rightarrow (D\text{-}A^{-}\text{-}D^{+}$ or $D^{+}\text{-}A^{-}\text{-}D)$ and the appearance of an ICT band at 770 nm.

Furthermore, the intense emission band at 700 nm in TRES with a lifetime of 2240 ps could be associated with the photogeneration of a polaron in the carbon chain [15]. In polyene structures, the initial excitation of the molecule occurs due to molecular excitons formed on the double bonds of the carbon chain. Such excitons rapidly self-localize and can be associated with the 690 nm band in the TRES at the initial excitation moment for both **PyC** and **BIC** dyes.

Thus, the results of combined quantum-chemical and spectral studies of the **PyC** and **BIC** dyes in a polar solvent allow us to stress that there are three relaxation pathways in the excited state:

symmetric (polymethine relaxation) pathway with alignment of bond lengths producing PL in the range of 700 and 730 nm for **BIC** and **PyC**, respectively; **polaron model** of a symmetrical form of the dye (large radius polaron inside the carbon chain) capable of transforming into a nonsymmetric form.

nonsymmetric (polyene) path - with a significant alternation of bond lengths and **exciton model** applied. PL emission in the range of

680–720 nm for **PyC** and 680–690 nm for **BIC** with relatively short lifetime; nonsymmetric dye form associated with charge localization on one of the TG and carbon chain.

donor-acceptor (D-A) path - relaxation of excitation in a nonsymmetric polyene form due to the electron density donating TG and a change in the direction of the dipole moment of the chain (from perpendicular to parallel). The characteristic PL range is 760–800 nm in BIC dye.

The above model can be represented in the form of an energy diagram (Fig. 6) with the relaxation processes indicated on it for **BIC** dye. λ_{EX} represent PL excitation in the range of absorption peak and corresponding PL pathways. Such paths are confirmed by the presence of various emission components in the TRES spectra at low temperatures. The proposed model can characterize the excited states in the pentamethine cyanine dyes and beyond explaining the impact of TG on spectral and lifetime features of fluorescence of such dyes. This model provides novel insight to the symmetric and non-symmetric forms of cationic cyanines [15] having a focus on how TGs affect the localization of this cation and emergence of new fluorescence in long-wavelength (NIR) range. In future, more comprehensive range of various TGs (cationic and anionic) needs to be studied with time-resolved techniques focusing on charge localization.

Better understanding of electron density donating TG impact will help in the design of molecules with large dipolar moment in excited state enabling two-photon absorption, up-conversion, energy transfer, bioimaging [35] etc. Another important aspect for modelling of such linear molecules with ICT is gaining insight into excited state dynamics of carotenoids [36,37], which participate in the process of photosynthesis. Such in-depth understanding of complex biological systems using simple modelling molecules paves the way towards development of efficient energy transfer systems for artificial photosynthesis.

4. Conclusion

The symmetry of the PMD molecule and localization of the excess charge on the carbon chain and terminal groups of the molecule can be different for its ground and optically excited states depending on the topology of the terminal groups, the polarity of the solvent, and the temperature. As a result, polyene, polymethine, or donor-acceptor structures can be formed for PMD molecules in molecular solutions, both in the ground state and in optically excited states.

To sum up, low-temperature spectral and quantum-chemical studies of cationic polymethine dyes showed the influence of terminal group electron density donating on relaxation of excited states. Depending on the topology of the terminal groups, the polarity of the solvent, and the temperature, the polyene or polymethine structure may predominate in the studied molecules. For the dye molecule with pyrylocyanine (**PyC**) terminal groups having low ability of the electron density transfer to the main polymethine chain, polyene relaxation pathway is possible in addition to the predominant polymethine pathway. Such polyene pathway is more efficient in the nonpolar environment of toluene and have small contribution in the polar acetonitrile. At low-temperatures for this dye, the absorption in electron-vibrational 0–1 transition has band broadening with intensity increase and 690 nm PL band in anti-Stokes range of polymethine maximum is observed which can be associated with the existence of dye molecules with broken symmetry in frozen solutions.

The benzo[*e*]indocarbocyanine (**BIC**) dye with a localized positive charge on the terminal groups has a negative charge transferred from terminal group to the polymethine chain leading to formation of donor-acceptor-donor system. **BIC** dye features with additional relaxation pathway in the excited state having characteristic emission in the range of 760–800 nm and relatively long lifetime. Besides, **BIC** dye at low temperature features predominantly polyene structure with strong contribution of 690 nm PL emission. Thus, the relaxation process of the donor-acceptor system, associated with charge transfer through the carbon chain and terminal groups, depends significantly on the chain features. For a well-conjugated cyanine chain structure, this process is characterized by short lifetimes. For the polyene structure, due to its dielectric-like properties, the process of emissive relaxation will be accompanied by long delay times after optical excitation.

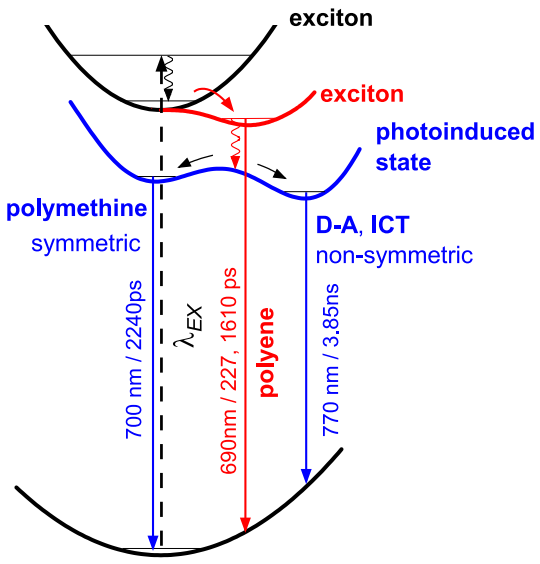

Fig. 6. Energy diagram for relaxation pathways of excited states with various τ and λ_{EM}. The characteristic lifetimes and emission wavelength are provided for **BIC** dye.

To sum up, at room temperature, the studied dyes, regardless of the symmetry in the ground state, are close to symmetric form in the excited state, and their spectral properties are determined by the degree of alignment of the C - C bonds and the distribution of charges on the carbon atoms in the carbon chain. At low temperatures, studied cationic dyes exhibit charge localization effects and their spectral properties can be associated with symmetry breaking in both the ground and excited states. Important insight has been gained in understanding features of terminal group and enabling us to advance on the design and synthesis of novel photoactive systems with predictable localization of cationic charge and functional features.

CRediT authorship contribution statement

Yuri Piryatinski: Writing – review & editing, Writing – original draft, Validation, Supervision, Methodology, Investigation, Funding acquisition, Formal analysis, Data curation, Conceptualization. **Anatoly Verbitsky:** Writing – review & editing, Writing – original draft, Visualization, Formal analysis, Conceptualization. **Markiian Malynovskyi:** Investigation, Data curation. **Aleksey Rozhin:** Resources, Methodology, Investigation. **Oleksiy Kachkovsky:** Writing – original draft, Validation, Supervision, Software, Methodology, Investigation, Formal analysis, Conceptualization. **Kateryna Maiko:** Writing – original draft, Visualization, Validation, Software, Investigation, Formal analysis, Data curation. **Yuri Slominskii:** Resources, Methodology, Investigation. **Petro Lutsyk:** Writing – review & editing, Writing – original draft, Visualization, Investigation, Formal analysis, Data curation, Conceptualization.

Declaration of competing interest

The authors declare that they have no known competing financial interests or personal relationships that could have appeared to influence the work reported in this paper.

Acknowledgements

Yu.P. acknowledges funding from the National Research Foundation of Ukraine (project #2022.01/0011).

Appendix A. Supplementary data

Supplementary data to this article can be found online at https://doi.org/10.1016/j.chemphys.2025.112620.

Data availability

Data will be made available on request.

References

[1] B. Valeur, *Molecular Fluorescence. Principles and Applications*; Wiley-VCH, Weinheim – New York – Chichester – Brisbane – Singapore – Toronto, 2001.
[2] A. Mezzetti, J. Schnee, A. Lapini, M. Di Donato, Photochem. Photobiol. Sci. 21 (2022) 557.
[3] G. Bach, S. Daehne, in: M. Sainsbury (Ed.), Cyanine Dyes and Related Compounds. ROOD'S Chemistry of Carbon Compounds. 2nd suppl. to 2nd ed., Vol. IVB, Het. Comp, Elsevier Science, Amsterdam, 1997, pp. 383–481.
[4] S.S. Matikonda, G. Hammersley, N. Kumari, L. Grabenhorst, V. Glembockyte, P. Tinnefeld, J. Ivanic, M. Levitus, M.J. Schnermann, J. Organomet. Chem. 85 (9) (2020) 5907.
[5] J.L. Bricks, A.D. Kachkovskii, Yu.L. Slominskii, A.O. Gerasov, S.V. Popov, Dyes Pigments 121 (2015) 238.
[6] S. Pascal, S.-H. Chi, J.W. Perry, C. Andraud, O. Maury, ChemPhysChem 21 (2020) 2536.
[7] H. Mustroph, Dyes Pigments 208 (2023) 110783.
[8] L.M. Tolbert, Acc. Chem. Res. 25 (12) (1992) 561.
[9] J.S. Craw, J.R. Reimers, G.B. Bacskay, A.T. Wong, N.S. Hush, Chem. Phys. 167 (1–2) (1992) 77.
[10] W. Xu, E. Leary, S. Sangtarash, M. Jirasek, M.T. González, K.E. Christensen, L. Abellán Vicente, N. Agraït, S.J. Higgins, R.J. Nichols, C.J. Lambert, H. L. Anderson, J. Am. Chem. Soc. 143 (48) (2021) 20472.
[11] A.D. Kachkovskii, Theor. Exp. Chem. 41 (3) (2005) 139.
[12] A.E. Masunov, D. Anderson, A.Ya. Freidzon, A.A. Bagaturyants, J. Phys. Chem. 119 (26) (2015) 6807.
[13] S.V. Vasylyuk, V.M. Yashchuk, O.O. Viniychuk, Yu.P. Piryatinski, M. M. Sevryukova, A.O. Gerasov, K.V. Zyabrev, Yu.P. Kovtun, M.P. Shandura, O. D. Kachkovsky, Mol. Cryst. Liq. Cryst. 535 (1) (2011) 123.
[14] P. Lutsyk, Yu. Piryatinski, O. Kachkovsky, A. Verbitsky, A. Rozhin, J. Phys. Chem. A 121 (43) (2017) 8236.
[15] Yu.P. Piryatinski, A.B. Verbitsky, A.M. Dmytruk, M.B. Malynovskyi, P.M. Lutsyk, A. G. Rozhin, O.D. Kachkovsky, Ya.O. Prostota, V.V. Kurdyukov, Dyes Pigments 193 (12) (2021) 109539.
[16] F. Terenziani, O.V. Przhonska, S. Webster, L.A. Padilha, Yu.L. Slominsky, G. Davydenko, A.O. Gerasov, Yu.P. Kovtun, M.P. Shandura, A.D. Kachkovski, D. J. Hagan, E.W. Van Stryland, A. Painelli, J. Phys. Chem. Lett. 1 (12) (2010) 1800.
[17] K.O. Maiko, I.M. Dmitruk, N.V. Obernikhina, A.D. Kachkovsky, Monatsh. Chem. 151 (2020) 559.
[18] A.D. Kachkovski, A.I. Tolmachev, Yu.L. Slominski, M.A. Kudinova, N. A. Derevyanko, O.O. Zhukova, Dyes Pigments 64 (3) (2005) 207.
[19] Yu.P. Piryatinski, A.B. Verbitsky, P.M. Lutsyk, A.G. Rozhin, O.D. Kachkovskii, Ya. O. Prostota, V.S. Brovarets, V.V. Kurdyukov, Mol. Cryst. Liq. Cryst. 672 (2018) 33.
[20] Revision A. Gaussian, M.J. Frisch, G.W. Trucks, H.B. Schlegel, H.B. Scuseria, M. A. Robb, et al., Gaussian, Inc, Wallingford CT, 2016.
[21] O.S. Nychyporenko, O.P. Melnyk, O.O. Viniychuk, T.M. Pinchuk-Rugal, V. A. Brusentsov, E.L. Pavlenko, O.P. Dmytrenko, N.P. Kulish, O.D. Kachkovsky, Int. J. Quantum Chem. 114 (2014) 416.
[22] Y. Zhao, D.G. Truhlar, Acc. Chem. Res. 41 (2) (2008) 157.
[23] D. Jacquemin, Ya. Zhao, R. Valero, C. Adamo, I. Ciofini, D.G. Truhlar, J. Chem, Theory Comput. 8 (4) (2012) 1255.
[24] A.A. Ishchenko, *Structure and spectral-luminescent properties of polymethine dyes.* Naukova Dumka: Kyiv, Ukraine, 1994.
[25] A.B. Ryabitsky, A.D. Kachkovski, O.V. Przhonska, J. Mol. Struct. (THEOCHEM) 802 (2007) 75.
[26] J.T. Gamel, A. Saxena, I. Batistic, A.R. Bishop, S.R. Philpot, Phys. Rev. B 45 (1997) 6408.
[27] K. Prassides, P.N. Schatz, K.Y. Wong, P.Z. Day, J. Phys. Chem. 90 (1986) 5588.
[28] T.D. Iordanov, J.L. Davis, A.E. Masunov, A. Levenson, O.V. Przhonska, A. D. Kachkovski, Int. J. Quantum Chem. 109 (2009) 3592.
[29] M. Eskandari, J.C. Roldao, J. Cerezo, B. Milián-Medina, J. Gierschner, J. Am. Chem. Soc. 142 (6) (2020) 2835.
[30] S. Pascal, A. Haefele, C. Monnereau, A. Charaf-Eddin, D. Jacquemin, B. Le Guennic, C. Andraud, O. Maury, J. Phys. Chem. A 118 (23) (2014) 4038.
[31] A.S. Tatikolov, L.A. Shvedova, J. Appl. Spectrosc. 85 (5) (2018) 693.
[32] O.P. Dimitriev, Chem. Rev. 122 (2022) 8487.
[33] E.I. Rashba, M.D. Sturge, Excitons, Modern Problems in Condensed Matter Sci (1982), https://doi.org/10.1002/bbpc.19840880428.
[34] J. Tan, D. Li, J. Zhu, N. Han, Y. Gong, Y. Zhang, Nanoscale 14 (2022) 16394.
[35] A. Martin, P. Rivera-Fuentes, Nat. Chem. 16 (2024) 28.
[36] L. Fiedor, A. Dudkowiak, M. Pilch, J.R. Soc, Interface 16 (2019) 20190191.
[37] K. Horiuchi, C. Uragami, R. Tao, D. Kosumi, R.J. Cogdell, H. Hashimoto, Molecules 28 (2023) 4424.